TELKOMNIKA Indonesian Journal of Electrical Engineering
Vol.12, No.2, February 2014, pp. 1374 ~ 1384
DOI: http://dx.doi.org/10.11591/telkomnika.v12i2.3904

Super-resolution Imaging Realization of Costas Signal

Wang Liang*, Shang Chao-xuan, He Qiang, Han Zhuang-zhi, Wang Yong-lei
Department of Electronics and Optics Engineering, Mechanical Engineering College,
Shijiazhuang 050003, Hebei, China
*Corresponding author, e-mail: kevin20911@163.com, junweilvmec@163.com

Abstract

Although the ambiguity function of Costas-coded FH (frequency hopping) signal has a thumbtack nature, its resolution in range and velocity domain is constraint by the bandwidth and time duration also. If one target is much stronger than the others in multi-targets detection environment, the sidelobes pedestal will make possible masking via the traditional stretch signal processing. Based on the diffraction model of radar target, sparse decomposition and compressed sensing are applied to reconstruct the radar range-velocity profiles with super-resolution. In order to get the super-resolution profiles, a sparse dictionary is constructed based on the Costas echo model, different sparsity measure functions are studied, and the penalizing function method and the Lagrangian multipliers method are introduced to get the optimal result. Some schemes are introduced to get the optimal atom and the differences between these schemes are compared via simulations.

Keywords*: costas-coded, sparse decomposition, compressed sensing*

1. Introduction

Costas-coded FH signal has good performance of range and velocity measurement. The ambiguity function of Costas-coded FH signal has a thumbtack nature, the main lobe is high and sharp, and the sidelobes are low and flat. So Costas-coded FH signal has no delay-Doppler coupling and can achieve super resolution of range and velocity [1]. Costas signal is very sensitive to velocity changes, velocity will make phase noise enhance and range profile attenuate sharply, the range profile will be submerged by the phase noise when the velocity is larger than the resolution. Therefore, velocity compensation becomes the key point of imaging. Many people have done a lot of researches on this problem. A continuous-wave (CW) signal was used as one of the probing signals along with the Costas signal in [2], and the CW signal is used just for the Doppler detection. A modified Costas signal in time and frequency is discussed in [3] to improve the ambiguity function performance. Different modulation effection between sub-pulses of Costas signal are presented and compared. A modified stretch processing was proposed in [4] based on high velocity targets detection in wideband environment. Stretch processing couldn't finish complete compensation at the same time when there are many targets with different velocities, inaccuracy compensation will make the sidelobes pedestal arise and possible masking when a target's RCS (Radar Cross Section) is much stronger than the others [5]. When the code is not long enough, this influence will be much more serious. One novel method to construct extended Costas sequences with ideal auto- and cross-ambiguity functions is proposed by combining the Golomb rulers with frequency hop sequences [6]. In order to reduce the sidelobes volume in ambiguity function, there are also many people beginning to study compound signal combining Costas signal and other modulations [7, 8] such as phase and frequency code during these years.

Sparse decomposition picks optimal elements from an overcomplete dictionary to represent the known signal, and it has attracted wide attention in many fields such as spectrum estimation [9], signal recovery [10], radar imaging [11] and so on in recent years. The ambiguity function of Costas signal has a thumbtack nature, although it can achieve high range and velocity resolution at the same time, the resolution is restricted by time and band width. Echoes from moving targets are related to several scattering points with fixed ranges and velocities, so they are sparse in range-velocity domain basically. With the help of sparse decomposition, a super-resolution imaging in rang-velocity domain is potential. Suppose signal has a sparse

Received July 15, 2013; Revised September 2, 2013; Accepted September 18, 2013

representation in some orthonormal basis, it can be reconstructed from smaller measurement via compressed sensing (CS) processing [12]. The CS theory has been used in many areas such as radar [13] and medical researches [14]. Based on the moving-targets echo model of Costas signal, the dictionary construction method and sparsity measure functions are studied in this paper. The super-resolution realization schemes using sparse decomposition and compressed sensing are compared via different optimization methods and the difference between the schemes are studied via simulaition.

2. Traditional Stretch Signal Processing

2.1. Costas-coded FH Radar Signal Model

Radar transmits Costas-coded FH signal with carrier frequency f_0, the time-frequency pulse train of this signal is shown in Figure 1, and the normalize complex expression is

$$S_T(t)=\sum_{i=0}^{N-1}\mathrm{rect}\left(\frac{t-T/2-iT_r}{T}\right)\exp\left[-j\cdot 2\pi\left(f_0+C_i\cdot\Delta f\right)t\right] \tag{1}$$

Where T is the pulse duration, T_r is the pulse repetition interval (PRI), Δf is the frequency step, and N is the pulse train number.

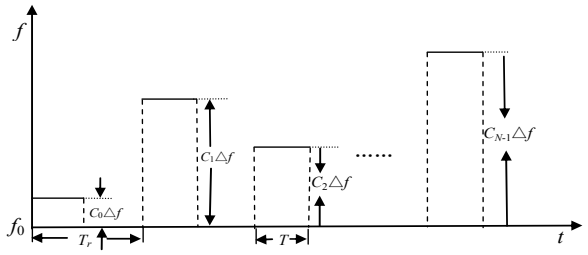

Figure 1. Costas-coded FH Pulse Train

The echo delay is:

$$\tau(t)=2(r-vt)/c \tag{2}$$

Where r and v denote the radial velocity and range when the first pulse is transmitted. The reference signal is:

$$S_0(t)=\sum_{i=0}^{N-1}\exp(j2\pi C_i\cdot\Delta ft)\exp(j2\pi f_0 t) \tag{3}$$

Echo mixes with the reference signal and the complex envelope of the mixer output is:

$$S_V(t)=\sum_{i=0}^{N-1}\mathrm{rect}\left[\frac{t-T/2-iT_r-2\left(r-vt\right)/c}{T}\right]\sigma\exp\left[-j\cdot 2\pi\left(f_0+C_i\cdot\Delta f\right)\cdot\frac{2\left(r-vt\right)}{c}\right] \tag{4}$$

Where σ is the scattering intensity. Sample echo at $t(i)=iT_r+T/2+2R/c$, then decode and normalize the sampling data, we get:

$$S_V'(i)=\sigma\exp\left\{-2\pi j\left(f_0+i\Delta f\right)\left[\frac{2r}{c}-\frac{2v}{c}\left(C_i'T_r+T/2+2r/c\right)\right]\right\}\qquad i=0,1,\cdots N-1 \tag{5}$$

Where C_i' is the decode number of i. According to (5), the echo phase is:

$$\theta'(i) = -2\pi\left(f_0 + i\Delta f\right)\left[\frac{2r}{c} - \frac{2v}{c}\left(C_i'\ T_r + T/2 + 2r/c\right)\right] \quad i = 0,1,\cdots N-1 \tag{6}$$

If the velocity is 0 m/s, the range profile is got after performing an IDFT. Suppose target travelling with a fixed velocity, $\theta'(i)$ will be decomposed into the following three parts ignoring the constant parts.

$$\theta_1'(i) = -2\pi i\Delta f\frac{2r}{c} \quad i = 0,1,\cdots N-1 \tag{7}$$

$$\theta_2'(i) = 2\pi i\Delta f\left(\frac{vT}{c} + \frac{4vr}{c^2}\right) \quad i = 0,1,\cdots N-1 \tag{8}$$

$$\theta_3'(i) = 2\pi\left(f_0 + i\Delta f\right)\left(\frac{2v}{c}C_i'\ T_r\right) \quad i = 0,1,\cdots N-1 \tag{9}$$

Here θ_1' is the phase related to the range of targets, after performing an IDFT, the output peaks indicate the range information. The pulse duration T is at the "μs" level and c is the velocity of light, so $\theta_2' \square\ \theta_1'$. The phase relationship in θ_3' is disturbed by the decode algorithm, and its IDFT output is just noise like. Based on the IDFT property, the IDFT output of θ_3' will convolute with the IDFT output of θ_1', and convolution algorithm results no range profile position changes but amplitude decay.

2.2. Traditional Stretch Signal Processing

The ambiguity function is a major tool to study and analyze radar signals. The ambiguity function of Costas FH signal has a thumbtack nature and the sidelobes will decay as the code length increases. Although the analytic ambiguity function of Costas FH pulse train is given in [15], the numerical form is always used as the analytic one is too complex. Zero-delay cut of AF is always used to analyze the velocity resolution. Set τ =0, and then:

$$\left|\chi(0,v)\right| = \left|\int_{-\infty}^{\infty} x(t)x^*(t)\exp(j2\pi vt)dt\right| \tag{10}$$

Zero-delay cut of AF shows that the velocity resolution has no relationship with the modulation mode but the complex envelop of the signal. According to the stepped-frequency pulse train given in [15], the velocity resolution of Costas FH signal is:

$$\Delta v = \frac{\lambda}{2NT_r} = \frac{c}{2f_0NT_r} \tag{11}$$

The traditional stretch signal processing of Costas signal is shown in Figure 2 [5]. Radar receiver samples echo data and gets N digital signal S_V, S_V is fed to a single IFFT block (after weighting) to yield a response matched to zero Doppler. The operation performed in the block marked diag(S_V)×MTX_n is used to generate many versions of vector S_V, each one compensates a different Doppler shift. Each row is identically processed by adding weights and performing an IFFT, and each row in the resulted complex array is a different Doppler-compensated version of S_V.

The range and velocity resolution of traditional stretch signal processing is limited by the bandwidth and duration of transmitting signal, targets whose range and velocity distinction are less than the resolution will not be distinguished via this processing.

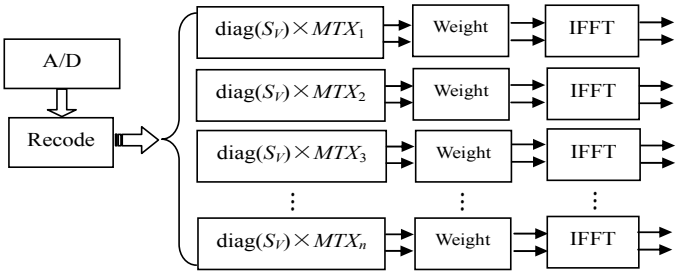

Figure 2. Stretch Signal Processing Method

3. Research Method

Based on the moving target echo model of Costas FH signal, a super-resolution realization is studied, an optimization algorithm is designed to get super-resolution image in range-velocity domain.

3.1. Basic Sparse Decomposition and Compressed Sensing Theory

Calculation and experiments show that echo energy reflected from target is related to some local scattering points, and this is a primary character when the transmitting frequency is high. The scattering points have their own fixed range and velocity value, it is sparse in range-velocity domain and this is just the theoretical basis of sparse decomposition. Set $\boldsymbol{S} \in \boldsymbol{R}^N$ as a signal measurement, if there is a coefficient vector $\boldsymbol{\alpha} \in \boldsymbol{R}^M$ (named as atom) fulfills that:

$$\boldsymbol{\Phi\alpha}=\boldsymbol{S} \tag{12}$$

Where $\boldsymbol{\Phi} = [\boldsymbol{\Phi}_0, \boldsymbol{\Phi}_1, \cdots \boldsymbol{\Phi}_{M-1}]$ is an overcomplete set (named as dictionary), $\boldsymbol{\Phi}_i \in \boldsymbol{R}^N$, i=0, 1,…, M-1, $\text{rank}(\boldsymbol{\Phi})=N<M$, $\boldsymbol{\alpha}$ is called an expression of $\boldsymbol{S}$ in dictionary $\boldsymbol{\Phi}$ [16]. The equality (12) has many solutions, and we need some additional information in order to get the unique one. The solution vector with a small number of nonzero elements is called a sparse one. If the atom is spare essentially, this priori information can be used to make up for the inadequate measurements. Sparse decomposition is used to search for a coefficient vector $\boldsymbol{\alpha}$ which has the least nonzero elements, namely:

$$\boldsymbol{\alpha}=\arg\min\|\boldsymbol{\alpha}\|_0 \quad \text{s.t.} \quad \boldsymbol{\Phi\alpha} = \boldsymbol{S} \tag{13}$$

This is a NP problem and not robust, and a sparsity measure function $d(\boldsymbol{\alpha})$ approximating $\|\boldsymbol{\alpha}\|_0$ is typically used to get the sparsest solution.

If the signal is sparse in some dictionary $\boldsymbol{\Phi}$, based on the CS theory, the sampling system can recover the signal with a very less measurements. In the standard CS theory [17], we acquire signal with the linear measurements.

$$\boldsymbol{Y}=\boldsymbol{\Psi S}=\boldsymbol{\Psi\Phi\alpha} \tag{14}$$

Where $\boldsymbol{\Psi}$ is an M_0×N matrix, M_0 □ N, and $\boldsymbol{Y}$ is the vector of measurements. The sparsity is the precondition of CS processing. There are many sampling matrixes can be used to get the measurements, we choose a random Gaussian matrix [18] to resample the echo in the next simulation. Using the sparse decomposition or CS processing, a super-resolution image in range-velocity domain may be reconstructed via constructing a dictionary and designing effective algorithm.

3.2. Sparse dictionary construction

Following (5) the echoes reflected from Q scattering points can be expressed as:

$$S'_V(i)=\sum_{q=1}^{Q}\sigma_q\delta\left(r_q,v_q\right)\exp\left[2j\pi\left(\frac{2v_q}{c}f_0C'_iT_r\right)\right]\exp\left[-2j\pi\left(i\Delta f\frac{2r_q}{c}\right)\right],\quad i=0,1,\cdots N-1 \qquad (15)$$

Where σ_q is the scattering intensity of the q-th scattering point, $\delta\left(r_q,v_q\right)$ is the remaining item related to r and v. Based on the analysis in [15], the unambiguity range of Costas-coded signal is $r_A=c/2\Delta f$, the range resolution is $\Delta r=c/2N\Delta f$, the unambiguity velocity is $v_A=c/2\Delta f$ and the velocity resolution is $v_A=c/2f_0T_r$. If we want to improve the range and velocity resolution to $\Delta r'=c/2M\Delta f$ and $\Delta v'=c/2f_0(2L+1)T_r$, where $M \gg N$, $2L+1 \gg N$, a dictionary $\boldsymbol{\Phi}=\left[\boldsymbol{\Phi}_{-L},\boldsymbol{\Phi}_{-L+1},\cdots\boldsymbol{\Phi}_{L-1},\boldsymbol{\Phi}_{L}\right]$ needs to be constructed based on the echo model, where:

$$\boldsymbol{\Phi}_l=\left[\boldsymbol{\varphi}_0^{(l)},\boldsymbol{\varphi}_1^{(l)},\cdots\boldsymbol{\varphi}_{M-1}^{(l)}\right],$$
$$\boldsymbol{\varphi}_m^{(l)}=\left[\phi_0^{(l,m)},\phi_1^{(l,m)},\cdots\phi_{N-1}^{(l,m)}\right]^T,$$
$$\phi_n^{(l,m)}=\exp\left(2j\pi\frac{l}{2L+1}C'_n\right)\exp\left(-2j\pi n\frac{m}{M}\right),$$

$l\in[-L, L]$, $m\in[0, M-1]$. The vector related to the two-dimensional super resolution image can be expressed as $\boldsymbol{\alpha}=[\boldsymbol{\alpha}_{-L}^T,\boldsymbol{\alpha}_{-L+1}^T,\cdots\boldsymbol{\alpha}_{L-1}^T,\boldsymbol{\alpha}_L^T]^T$, where $\boldsymbol{\alpha}_l=[\alpha_0^l,\alpha_1^l,\cdots,\alpha_{M-1}^l]^T$ is the range profile at the l-th velocity cell. The final range-velocity image is obtained by reshaping $\boldsymbol{\alpha}$ .Notice that the range in the m-th range cell is $r_m=m*\Delta r'$, the velocity in the l-th velocity cell is $v_l=l*\Delta v'$, and the absolute value of $\boldsymbol{\alpha}$ are just the scattering intensity in different cells.

3.3. Sparsity Measure Function Construction

The best measure function $F(\boldsymbol{\alpha})$ is the l_0 norm, as it is very difficult to get the resolution based on the analysis in 3.1, many other functions such as $l_{p\le1}$ norm, logarithmic function and so on are used instead of l_0 norm. The measure function needs to be concave in the first quadrant, and it is changeable and symmetric to every component [16]. A sparsity measure function used in [16] is shown in formula (16) here.

$$F(\boldsymbol{\alpha})=\sum_{i=0}^{N-1}\ln\left(1+\frac{|p_i|}{\beta}\right) \qquad (16)$$

where $p_i=|\alpha_i|/\|\boldsymbol{\alpha}\|$ and $\|\boldsymbol{\alpha}\|=\sum_{i=1}^{N}|\alpha_i|$, β is a constant value. Set parameters just like section 4 and β to be 0.001. Suppose there is a scattering point travelling with different velocities at a fixed range, calculate the sparsity of the echo according to (16), we get Figure 3. There are many local minimum and a global minimum along the velocity changes.

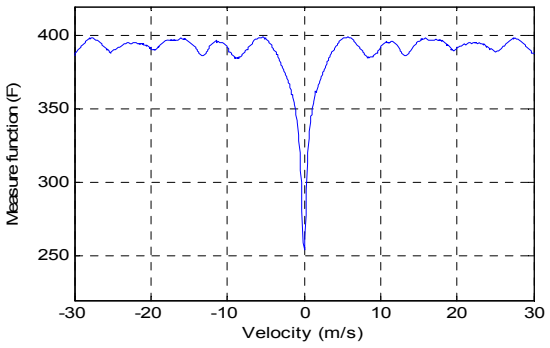

Figure 3. Sparsity Measure Function $F(\boldsymbol{\alpha})$

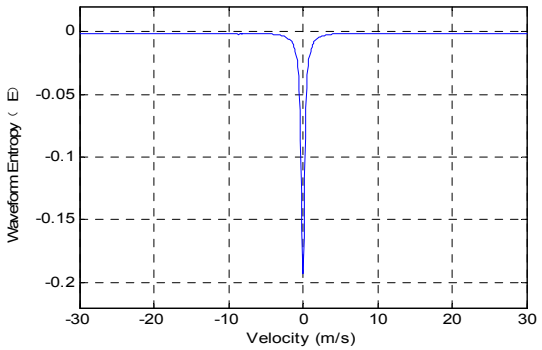

Figure 4. Waveform Entropy

Entropy is generally used to measure the uncertainty of random variable, here we difine a waveform entropy. Given a disperse sequence $\boldsymbol{\alpha}=\{\alpha_1, \ldots, \alpha_N\}$, the waveform entropy of $\boldsymbol{\alpha}$ is:

$$E(\boldsymbol{\alpha}) = A\sum_{i=1}^{N} p_i \lg(1-p_i) \qquad 0 \le p_i \le 1 \tag{17}$$

Where A is a constant value used to modulate the range of the waveform entropy, and p_i is defined just like (16). The waveform entropy is a measurement of the energy divergence degree along parameter axis, and it is used to measure the sparsity of the echoes in this paper. For a fixed waveform, the larger the entropy is, the more uniformity the waveform is. Set parameters as section 4 and A to be 1, here is a scattering point with fixed range but different velocities. Calculate the waveform entropy of the echo reflected from this point, we get Figure 4. The ordinate axis in Figure 4 is the waveform entropy and the lateral axis is the velocity. This simulation shows that the waveform entropy has a global minimum value when the velocity is zero along the velocity axis.

Based on the analysis in 2.2, we know that the range profile attenuates heavily and the energy diverges along the range axis when the target travelling velocity is larger than the resolution. Using waveform entropy to measure the divergence degree, the waveform entropy will become greater. We will get the minimum waveform entropy value if we make compensation with the right velocity. As the range profile diverges seriously, the sparsity of the corresponding range profile gets worse. Take the waveform entropy as the measure function, the waveform entropy value will represent the sparsity degree of the range profile. The atom get from the dictionary represents the range-velocity information of the scattering point, and the sparsest solution is the minimum value of the measure function. Let:

$$f(x) = Ax\lg(1-x) \qquad 0 \le x \le 1 \tag{18}$$

The second derivative of $f(x)$ is:

$$f''(x) = \frac{Ax}{(1-x)^2 \ln 10} \ge 0 \qquad 0 \le x \le 1 \tag{19}$$

So $f(x)$ is concave in the feasible set. $E(\boldsymbol{\alpha})$ is also a concave functional since it is a "sum" of function $f(x)$, and the local and the global minimum are the same.

3.4. Algorithm Design and Analysis

There are many methods have been proposed in solving the convex constrained optimization problem, such as gradient projection method [19], Compressive Sampling Matching Pursuit method (CoSaMP) [20] and so on. Here we get the optimal result with the help of gradient method. Choose a sparsity measure function, denote it as $F(\boldsymbol{\alpha})$:

$$F(\boldsymbol{\alpha}) = \sum_{i=0}^{M-1} \eta(\alpha_i) \tag{20}$$

Rewrite formula (13) as:

$$\boldsymbol{\alpha} = \arg\min F(\boldsymbol{\alpha}), \quad \text{s.t.} \quad h(\boldsymbol{\alpha}) = \left\| \boldsymbol{\Phi\alpha} - \boldsymbol{S} \right\|_2 = 0 \tag{21}$$

Translates formula (21) into an unconstrained optimization model using penalizing function method, we get:

$$\min J(\boldsymbol{\alpha}) = F(\boldsymbol{\alpha}) + \frac{M}{2}\left\| \boldsymbol{\Phi\alpha} - \boldsymbol{S} \right\|_2^2 \tag{22}$$

Where M>0 is the regularized parameter related to noise level. Newtonian iteration method [21]

is used to get the optimal solution of formula (22) and we get:

$$\boldsymbol{\alpha}_{k+1}=\boldsymbol{\alpha}_k-\gamma\cdot\left[\nabla^2 J(\boldsymbol{\alpha}_k)\right]^{-1}\cdot\nabla J(\boldsymbol{\alpha}_k) \tag{23}$$

Take γ=1, we get the special Newtonian iteration method. Now we just need to solve the gradient of the object function $J(\boldsymbol{\alpha})$. Base on (22), we get:

$$\nabla J(\boldsymbol{\alpha})=\nabla F(\boldsymbol{\alpha})+M\left[\boldsymbol{\Phi}^{\mathrm{T}}\boldsymbol{\Phi}\boldsymbol{\alpha}-\boldsymbol{\Phi}^{\mathrm{T}}\boldsymbol{S}\right] \tag{24}$$

Where $\nabla F(\boldsymbol{\alpha})=\mathrm{diag}\left\{\left[\frac{d\eta(\alpha_0)}{d\alpha_0},\frac{d\eta(\alpha_1)}{d\alpha_1},\cdots\frac{d\eta(\alpha_{N-1})}{d\alpha_{N-1}}\right]\right\}=\mathrm{diag}\left\{\frac{d\eta(\alpha_i)}{d\alpha_i}\right\}$.

Take another function $\eta_\varepsilon(t)=\eta(\sqrt{t^2+\varepsilon})$ to approximate $\eta(t)$, the derivative of $\eta_\varepsilon(t)$ is:

$$\frac{d\eta_\varepsilon(t)}{dt}=\left.\frac{d\eta(y)}{dy}\right|_{y=\sqrt{t^2+\varepsilon}}\cdot\frac{t}{\sqrt{t^2+\varepsilon}}=\eta'(\sqrt{t^2+\varepsilon})\cdot\frac{t}{\sqrt{t^2+\varepsilon}} \tag{25}$$

Make $\varepsilon\to 0^+$, (24) can be rewritten as:

$$\nabla J(\boldsymbol{\alpha})=\boldsymbol{\Pi}_k\cdot\boldsymbol{\alpha}+M\left[\boldsymbol{\Phi}^{\mathrm{T}}\boldsymbol{\Phi}\boldsymbol{\alpha}-\boldsymbol{\Phi}^{\mathrm{T}}\boldsymbol{S}\right] \tag{26}$$

Where $\boldsymbol{\Pi}_k=\mathrm{diag}\left\{\frac{\eta'(|\alpha_k|)}{|\alpha_k|}\right\}$. Further more, we can get:

$$\nabla^2 J(\boldsymbol{\alpha})=\boldsymbol{\Pi}_k+M\cdot\boldsymbol{\Phi}^{\mathrm{T}}\boldsymbol{\Phi} \tag{27}$$

Take (26) and (27) into (23), we get:

$$\left[\boldsymbol{\Pi}_k+M\cdot\boldsymbol{\Phi}^{\mathrm{T}}\boldsymbol{\Phi}\right]\boldsymbol{\alpha}_{k+1}=\left[\boldsymbol{\Pi}_k+M\cdot\boldsymbol{\Phi}^{\mathrm{T}}\boldsymbol{\Phi}\right]\boldsymbol{\alpha}_k-\left[\boldsymbol{\Pi}_k\cdot\boldsymbol{\alpha}_k+M\left(\boldsymbol{\Phi}^{\mathrm{T}}\boldsymbol{\Phi}\boldsymbol{\alpha}_k-\boldsymbol{\Phi}^{\mathrm{T}}\boldsymbol{S}\right)\right] \tag{28}$$

After simplification we get the generalized and regularized focal undetermined system solver (FOCUSS) iterative formula [16].

$$\boldsymbol{\alpha}_{k+1}=[\kappa\boldsymbol{\Pi}_k+\boldsymbol{\Phi}^{\mathrm{H}}\boldsymbol{\Phi}]^{-1}\boldsymbol{\Phi}^{\mathrm{H}}\boldsymbol{S} \tag{29}$$

where $\kappa=1/M$. After k_0 iterations, we get the optimal resolution $\boldsymbol{\alpha}_{k_0}^*$ of the unconstrained optimization model which should fulfill that

$$\nabla F(\boldsymbol{\alpha}_{k_0}^*)+\lambda^*\nabla h(\boldsymbol{\alpha}_{k_0}^*)=0 \tag{30}$$

Where λ* is a Lagrange multiplier, and it may not be zero every time, so the gradient of measure function $d(\boldsymbol{\alpha})$ is normally nonzero at the constraint minimal point. After k_0 iterations using penalizing function, the optimal solution $\boldsymbol{\alpha}_{k_0}^*$ fulfills that:

$$\nabla J(\boldsymbol{\alpha}_{k_0}^*)=\nabla F(\boldsymbol{\alpha}_{k_0}^*)+Mh(\boldsymbol{\alpha}_{k_0}^*)\nabla h(\boldsymbol{\alpha}_{k_0}^*)=0 \tag{31}$$

As $h(\boldsymbol{\alpha}_{k_0}^*)$=0, we get:

$$\nabla F(\boldsymbol{\alpha}_{k_0}^*)=0 \tag{32}$$

And this is contrary to the solution got from (30). For a given constrained problem, the penalizing function method may not get the optimal result after iterations unless the optimal solution $\boldsymbol{\alpha}_{k_0}^*$ is just in the feasible set. Based on the Lagrange multipliers method, translate formula (21) into an unconstrained optimization shown as:

$$\min J(\boldsymbol{\alpha}, \lambda', M') = F(\boldsymbol{\alpha}) + \lambda' h(\boldsymbol{\alpha}) + \frac{M'}{2} h^2(\boldsymbol{\alpha}) \tag{33}$$

Where λ' is the Lagrangian multiplier which ensures that the unconstraint solution fulfills the constraint condition. If $\boldsymbol{\alpha}_k^*$ is the optimal solution after the k-th iteration, and then:

$$\nabla F(\boldsymbol{\alpha}_k^*) + \left[\lambda_k' + M_k' h(\boldsymbol{\alpha}_k^*) \right] \nabla h(\boldsymbol{\alpha}_k^*) = 0 \tag{34}$$

So the Lagrange multiplier should follow (35) in the iterative operation.

$$\lambda_{k+1}' = \lambda_k' + M_k' F(\boldsymbol{\alpha}_k^*) \tag{35}$$

Based on the Newtonian iteration formula(23), the unconstrained optimization problem will converge to the optimal solution of the constraint problem rapidly. In order to optimize the dictionary, pulse accumulation is used to estimate the velocity firstly; then construct a dictionary around the estimated velocity, and the dictionary dimension, iteration and calculation amount will be substantially reduced.

4.Simulation Result

Set simulation parameters as: f_0=35 GHz, N=256, Δf=1 MHz, T=0.2 μs, T_r=10 μs. Base on the bandwidth and (11), we get the range and velocity resolution: Δr=0.59 m and Δv=1.67 m/s. Suppose a target consists of four scattering points as shown in Figure 5, and point 0 is at [500 120] m. There is 2m between the scattering point and its neighbors, the target travel with a initial velocity at [0, 10] m/s, and a radar is placed at [0 0] m. The scattering intensities of the scattering points flash randomly during the entire track. The initial ranges of the four scattering points are r_n =[514.42, 515.20, 513.84, 515.78] m, their corresponding velocities are v_n =[-2.23, -1.87, -2.03, -2.07] m/s and their scattering coefficients are σ_n=[1, 0.50, 0.07, 0.50].

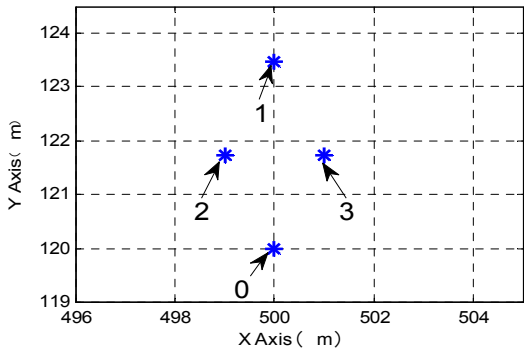

Figure 5. Scattering Points Model

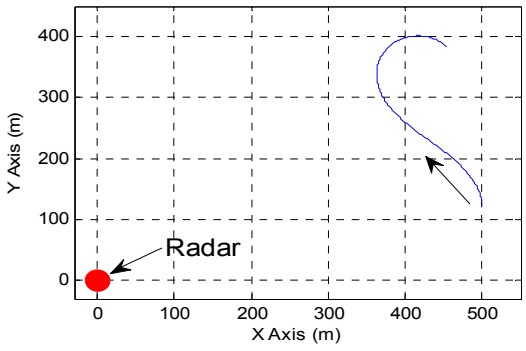

Figure 6. Travel Track of the Target

4.1 Comparison between Different Schemes used in Super-resolution Realization

Based on the analysis in 3.1, there are two processing methods in achieving the super-resolution result: the sparse decomposition and the CS processing; there are two measure functions are introduce in 3.2: a general used measure function $F(\boldsymbol{\alpha})$ and the waveform entropy function $E(\boldsymbol{\alpha})$; and two methods are studied to solve the optimization problem in 3.3: penalizing

function method and the Lagrangian multipliers method. Based on the all introduction above, we can get eight super-resolution schemes here:

(1) Sparse decomposition using measure function $F(\alpha)$ and penalizing function method (SFP);
(2) Sparse decomposition using measure function $E(\alpha)$ and penalizing function method (SEP);
(3) Sparse decomposition using measure function $F(\alpha)$ and Lagrangian multipliers method (SFL);
(4) Sparse decomposition using measure function $E(\alpha)$ and Lagrangian multipliers method (SEL);
(5) CS theory using measure function $F(\alpha)$ and penalizing function method (CFP);
(6) CS theory using measure function $E(\alpha)$ and penalizing function method (CEP);
(7) CS theory using measure function $F(\alpha)$ and Lagrangian multipliers method (CFL);
(8) CS theory using measure function $E(\alpha)$ and Lagrangian multipliers method (CEL);

The differences of the final super-resolution results getting from the eight schemes are not very obvious, so we analyse the realizated speed of different schemes and take the iterative steps as a standard. Carry on the simulation introduced in section 4.1 for 40 s via different schemes and save the iterative steps every time, we get results shown in Table 1 and Table 2.

Table 1. Iterative Steps of Different Schemes

Item	SFP	SEP	SFL	SEL	CFP	CEP	CFL	CEL
Max.	117	132	96	107	90	130	133	13
Min.	19	12	16	11	14	8	7	74
Average	44.4	40.2	32.5	29.1	31.1	31.8	26.0	25.4

Table 2. Average Iterative Steps of Different Schemes

Item	Sparse decomposition		Compressed sensing	
	Penalizing	Lagrangian	Penalizing	Lagrangian
$F(\alpha)$	44.4	32.5	31.1	26.0
$E(\alpha)$	40.2	29.1	31.8	25.4

Based on the results above, we get the following results:

(1) Based on the CS processing, we can get the super-resolution image and the program efficiency is better than the algorithm of sparse decomposition as the CS processing is carried on a much lower dimension;
(2) Waveform entropy used as a measure function has better performance than the one used in [16];
(3) The Lagrangian multipliers method convergence at a faster rate than the penalizing function method.

4.2. Comparison between Traditional Stretch Processing and Super-resolution Realization

Based on the stretch signal processing, we get the range-velocity domain image shown in Figure 7. There is only one peak in Figure 7 and the four scattering points could not be distinguished in range or velocity domain via this signal processing. Based on the super-resolution realization, a dictionary is constructed based on the target range profile firstly, there are eight schemes that can get the super-resolution result and take the eighth scheme, CEL, as an example. The sampling matrix $\boldsymbol{\Psi}$ is a 150×256 Gaussian random matrix, the parameter A used in $E(\alpha)$ is set to be 1500, the regularization parameter M' is set to be 1 and the Lagrangian multiplier λ' is set to be 0, then the optimal result is acquired as shown in Figure 8. Compared with Figure 7, Figure 8 gets a super-resolution image in the range-velocity domain, the peaks in the two-dimensional image reflect the range and velocity information rightly and the four scattering points are separated which could not be separated via stretch processing. The scattering intensity even the smallest one is shown, and this verifies the correctness of using the

super-resolution realization. Meanwhile, the dictionary construction errors between the real value and the measurement make energy leak to the nearby cells, the corresponding scattering coefficients of the scattering points attenuate by some degree which make some peaks appear at the corresponding positions.

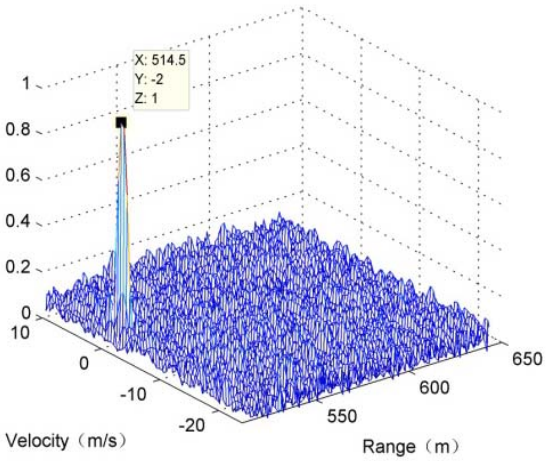

Figure 7. 2-D Image Via Stretch Processing

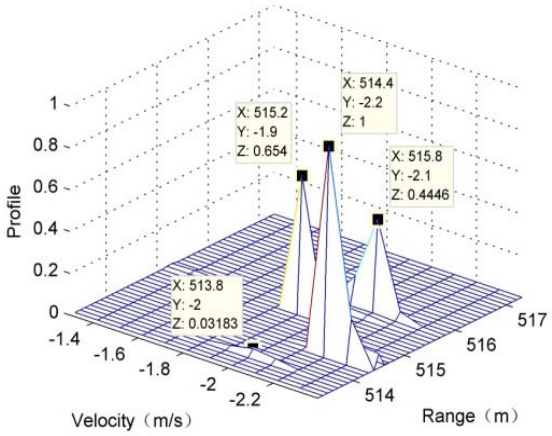

Figure 8. Super-resolutin Algorithm Result

Make this simulation go on for 40 s, the CEL algorithm is utilized during the whole track. The dictionary is constructed base on the former measurement, iteration begins and the super-resolution profiles are got finally based on this algorithm. The range and velocity errors between the real target position and the measurement are shown in Figure 9 and Figure 10. Compared with the range and velocity resolution discussed in 2.2, the errors are very small, and the errors in range and velocity domain using this algorithm are enhanced.

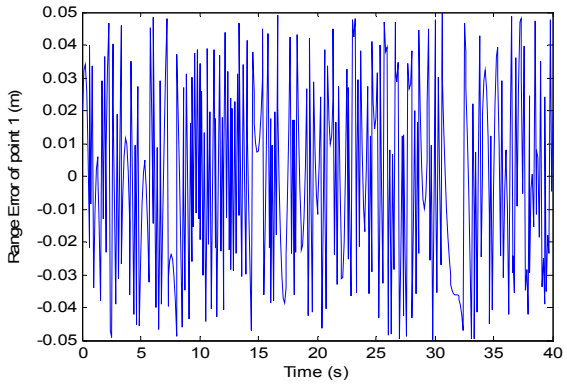

Figure 9. Range Error of Point 1

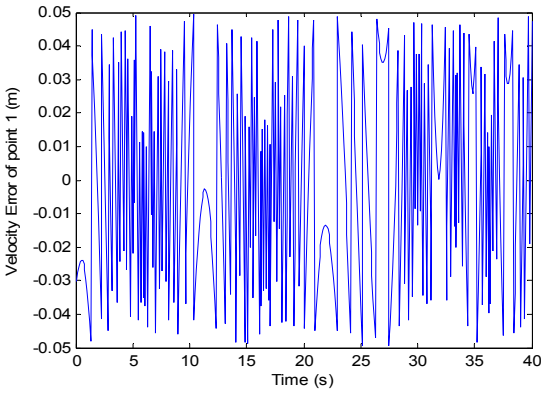

Figure 10. Velocity Error of Point 1

5. Conclusion

A super-resolution imaging of Costas FH signal is studied based on sparse decomposition and CS theory in this paper. With limited sampling rate, a super-resolution in range-velocity domain is realized. Using different measure functions and optimization methods, some possible schemes are designed, and the caculation difference between these schemes are compared via simulation. Take the CEL scheme as an example, the super-resolution image is compared with the traditional stretch processing. With range, velocity, and scattering intensity

accuratly detected, this algorithm has a very high application value in target identification. Also the high-speed algorithm needs to be further studied.

Acknowledgements

LiYue and WuRun are both first author,they have the equal amount of work, Huangyongppin is second anthour, Liang Wang is the corresponding author.

References

[1] CF Chang, MR Bell. Frequency-Coded Waveforms for Enhanced Delay-Doppler Resolution. *IEEE Transactions on Information Theory*. 2003; 49(11): 2960-2971.
[2] SK Mehta, EL Titlebaum. *A new method for measurement of the target and channel scattering functions using Costas arrays and other frequency hop signals*. Acoustics, Speech, and Signal Processing. 1991: 1337-1340.
[3] Kasas Khaola; Aboulnour Hassan, Kawas Osama. *Improving ambiguity function of Costas signal*. 2009 Mediterrannean Microwave Symposium. Piscataway. 2009: 1-5.
[4] Wei Xi-zhang, Liu Zhen,Deng-bin, Li Xiang. Research on Velocity Measurement of Wideband Costas-Coded Stepped-Frequency Radar Signal. *Acta Electronica Sinica*. 2010; 38(10): 2426-2429.
[5] N Levanon. *Stepped-frequency pulse-train radar signal*. IEE Proceedings-Radar, Sonar and Navigation. 2002; 149(6): 297-309.
[6] Chao-Chin Yang. *New extended Costas sequences with ideal auto-and cross-ambiguity functions*. 2009 International Conference on Communications, Circuits and Systems. 2009: 156-159.
[7] PE Pace, CY Ng. Costas CW frequency hopping radar waveform: peak sidelobe improvement using Golay complementary sequences. *Electronics Letters*. 2010; 46(2): 169-170.
[8] Zhen Liu, Bin Deng, Xi zhang Wei. *Modified stepped-frequency train of LFM pulses*. 2008 International Conference on Information and Automation. Zhangjiajie. 2008: 1137-1141.
[9] Md Mashud Hyder, Kaushik Mahata. Coherent Spectral Analysis of Asynchronously Sampled Signals. *IEEE Signal Processing Letters*. 2011; 18(2): 126-129.
[10] T Peleg, YC Eldar, M Elad. Exploiting Statistical Dependencies in Sparse Representations for Signal Recovery. *IEEE Transactions on Signal Processing*. 2012; 60(5): 2286-2303.
[11] DU Xiao-yong, HU Wei-dong, YU Wen-xian. Sparse representation technique for high range resolution profiles. *Systems Engineering and Electronics*. 2005; 27(6): 968-970,987.
[12] DL Donoho. Compressed Sensing. *IEEE Transactions on Information Theory*. 2006; 52(4): 1289-1306.
[13] Lingwen Zhang. Sparsity-based Angle of Arrival Estimation for Emitter Localization. *TELKOMNIKA Indonesian Journal of Electrical Engineering*. 2012; 10(4): 769-774.
[14] Windra Swastika, Hideaki Haneishi. Compressed Sensing for Thoracic MRI with Partial Random Circulant Matrices. *TELKOMNIKA Indonesian Journal of Electrical Engineering*. 2012; 10(1): 147-154.
[15] N Levanon, E. Mozesona. Radar Signals. New Jersey: John Wiley & Sons, Inc. 2004.
[16] DU Xiao-yong, HU Wei-dong, YU Wen-xian. Generalized regularized FOCUSS algorithm and its convergence analysis. *Systems Engineering and Electronics*. 2005; 27(5): 922-925.
[17] MA Davenport, PT Boufounos, MB Wakin, et al. Signal Processing With Compressive Measurements. *IEEE Journal of Selected Topics in Signal Processing*. 2010; 4(2): 445-460.
[18] Yaakov Tsaig, David L Donoho. Extensions of compressed sensing. *Signal Processing*. 2006; 86(3): 549-571.
[19] Mário AT Figueiredo, Robert D Nowak, Stephen J Wright. Gradient Projection for Sparse Reconstruction: Application to Compressed Sensing and Other Inverse Problems. *IEEE Journal of Selected Topics in Signal Processing.* 2007; 1(4): 586-597.
[20] Deanna Needell, Joel A Tropp. CoSaMP: Iterative signal recovery from incomplete and inaccurate samples. *Communications of the ACM*. 2010; 53(12): 93-100.
[21] Su Tashan. The Optimal Computer Principle and Algorithm Programming. Changsha, Hunan: *Journal of National University of Defense Technology.* 2001: 151-164.